Advances in the Control Schemes for MR Actuators

Gabriel Mendes
School of Technology and Management of Bragança
Polytechnic Institute of Bragança
Campus de Santa Apolónia, 5300-253, Bragança , Portugal
Email: gabriel.diasmendes@hotmail.com

Janusz Gołdasz*†
†*Faculty of Electrical and Computer Engineering*
Cracow University of Technology
ul. Warszawska 24, 32-155 Krakow, Poland
Email: jgoldasz@pk.edu.pl

**BWI, Technical Center Krakow*
ul. Medweckiego 2, 32-083 Balice, Poland

2022 23rd International Carpathian Control Conference (ICCC) | 978-1-6654-6636-3/22/$31.00 ©2022 IEEE | DOI: 10.1109/ICCC54292.2022.9805907

***Abstract*—Magnetorheological (MR) actuators are known semi-active devices. In the essence, the hardware incorporates a valve being a solenoid with a flow channel. Supplying the current to the solenoid's coil induces the magnetic field in the channel. As a results, the fluid transitions from a near-Newtonian one to a pseudo-solid. In the paper we show that significant improvements in the MR actuator dynamics can be achieved by exploring flux feedback control systems rather than current feedback ones. The flux-based approach would improve the system's response time and its bandwidth as well as minimize the contribution of the eddy currents. Thus, numerical simulations have been carried out to test the original hypothesis. The obtained data (from co-simulations) prove that the proposed approach delivers good results although further research is required on further optimizing the controller's gains and prior to building a real prototype.**

***Keywords*—magnetorheological actuator, response, dynamics, control**

I. Introduction

To begin with, magnetorheological (MR) fluids are representatives of smart materials. In the presence of external magnetic fields the materials develops a yield stress [1]. The technology has been researched and utilized commercially in controllable semi-active vehicle dampers or powertrain mounts. Contrary to conventional semi-active dampers in which flow restriction is developed by forcing the fluid via a variable area orifice, MR dampers are valveless. A typical MR actuator is structurally simple. It features a cylinder tube housing a solenoid assembly with a flow channel, a pressurized gas volume for volume compensation and electrical connections to the power supply on the car. Its operating principle is simple and relies on inducing magnetic flux of sufficient amplitude in the flow channel for energizing the fluid. As a result, the fluid develops a yield stress which again translates into a resistance-to-flow build up (damping force change). The transition is reversible and fast.

In general, various mechanisms make the process complex. Non-linear magnetisation characteristics of the materials in the solenoid's circuit, the yield stress dependance on the magnetic field, not to mention the solenoid's dynamics and controller's dynamics as well as mechanical hysteresis and magnetic hysteresis are among the key contributors to the flux-force conversion [2]–[4]. Hence, an efficient control scheme is obligatory for a successful MR application. For instance, Choi et al. [5] highlights fundamental requirements for a controller for use in MR systems, i.e. response time, robustness, control accuracy. However, due to the above, developing an optimal control algorithm for an MR system is difficult or impossible to obtain, and the controller choice seems to depend on particular application requirements. Only a brief review of MR applications reveals the use of PID (proportional-integral-derivative) controllers, sky-hook controllers, neural network control systems, fractional-order controllers or robust controllers (H-∞) [6]–[10]. However, a majority of control schemes rely on the current feedback information, thus ignoring the dynamics of the electromagnet (and the force dependence on the flux and not the current). There are notable exceptions, though. Nehl et al. [11] developed a flux-based control approach specifically dedicated to MR systems, and early on Yang [12] studied the response of a seismic system with a force controller.

To complement the outcome of these studies, the goal of the present study was to provide a basic insight into the MR control system response, develop a hybrid co-simulation control system, and then compare its outcome by analyzing various control schemes.

Briefly, in the study we present the results of a simulations in which the we examine various control scenarios and itheir impact on the actuator's dynamics (magnetic flux). In Section II we show crucial details of the examined MR actuator's geometry and material properties. Next, in Section III we describe the two control circuits examined in the paper, whereas in Section IV the numerical experiment results are presented. Finally, we summarize the results and draw conclusions in Section V.

II. MR Actuator

The analyzed MR valve is illustrated in Fig. 1. The FE (finite-element) transient model was prepared in Ansys Maxwell 2021R2 – see Fig. 1. The axi-symmetric model of the valve represents the configuration of a simple MR valve with one coil assembly and an annular flow channel. The two aluminum plates keep the sleeve in place.

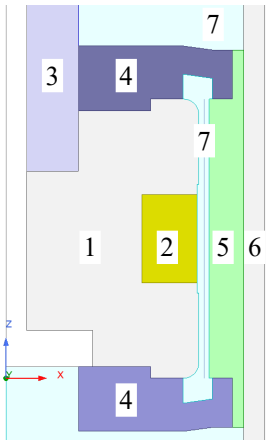

Fig. 1. Finite-element model of the MR actuator (Ansys Maxwell 2021 R2); 1 – solenoid core, 2 – coil, 3 – rod, 4 – non-magnetic plates, 5 – sleeve, 6 – cylinder, 7 – MRF

As shown, the valve's outer diameter is equal to 46 mm, and the rod's outer diameter is 14 mm. The flow channel's length is equal to 27 mm. The gap height is 1 mm. Moreover, the outside diameter of the core is equal to 37.3 mm. The coil window dimensions are: 9.25 mm wide by 5.5 mm deep. It accomodates 100 wire turns (size: 0.51 mm dia.) which results in the winding resistance equal to appr. 1 Ω.

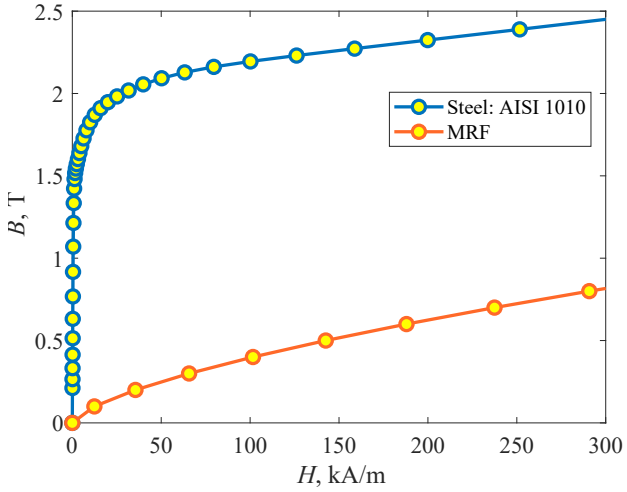

Fig. 2. Magnetisation ($B-H$) curves; B – magnetic flux density, H - magnetic field strength

Next, the MR fluid's properties are typical of a 26 percent Fe vol. MRF. The cylinder tube, the ring, the core are made of the AISI 1010 steel alloy, respectively, and the rod's material is AISI 4130. The magnetization curves are shown in Fig. 2. Finally, the electrical conductivity of the AISI 1010 material was assumed to be 5.8 MS/m, AISI 4130: 4.4 MS/m, Al: 37 MS/m. The model omits magnetic hysteresis, however, coil dynamics and eddy currents are accounted for in the simulations. The coil wiring is connected to the external voltage source.

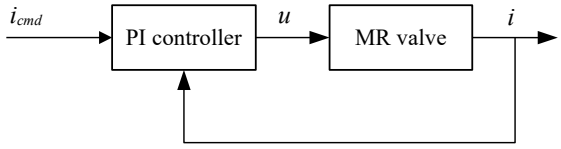

Fig. 3. Current controller layout; i_{cmd} – current command, u – voltage, i - coil current

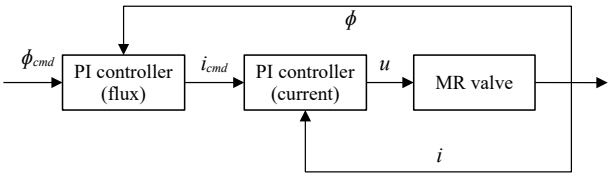

Fig. 4. Cascade controller layout; ϕ_{cmd} – magnetic flux command input, ϕ – magnetic flux

III. Control System

In this section the examined control circuits are presented in sections that follow below. First, the conventional PI current driver's diagram is highlighted to be followed then by the dual PI magnetic flux driver.

A. Current PI controller

The current controller of interest is a conventional PI analog controller with the current feedback loop – see Fig. 3. The reference signal that the driver receives is the current command input. Then, the output from the controller is converted into the constrained voltage input (±12.5 V). The PI driver is characterized by the proportional gain K_{pi} and the integral gain K_{ii}, respectively.

B. Cascade PI magnetic flux controller

The analyzed flux controller is a cascade controller composed of two analog PID drivers (see Fig. 4). In the essence, the controller is analogous to the driver proposed in [11], [13]. As shown, the first controller is the flux driver followed by the current driver. The reference input is a command signal corresponding to the desired flux level, and the computed flux is extracted from the FE model of the actuator. This way, the output of the first driver drives the current controller with the current input. Finally, the output of the last driver is the voltage applied to the coil winding. The current PI driver is characterized by the proportional gain K_{pi} and the integral gain K_{ii}, respectively, whereas the flux driver is referred to by the proportional gain K_{pf} and the integral gain K_{if}, respectively.

IV. Results

To accomplish the objectives, we developed a hybrid (co-simulation) model with Ansys Twin Builder and Ansys

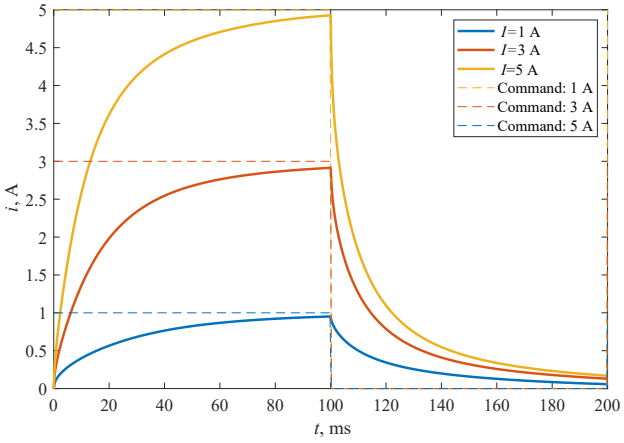

Fig. 5. Open loop: response to step voltage inputs – coil current

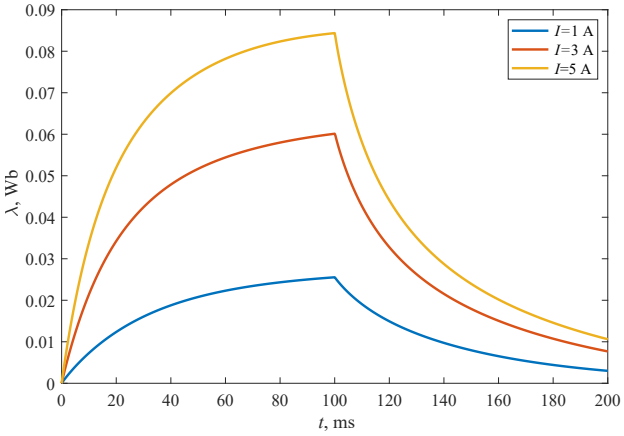

Fig. 6. Open loop: response to step voltage inputs – magnetic flux

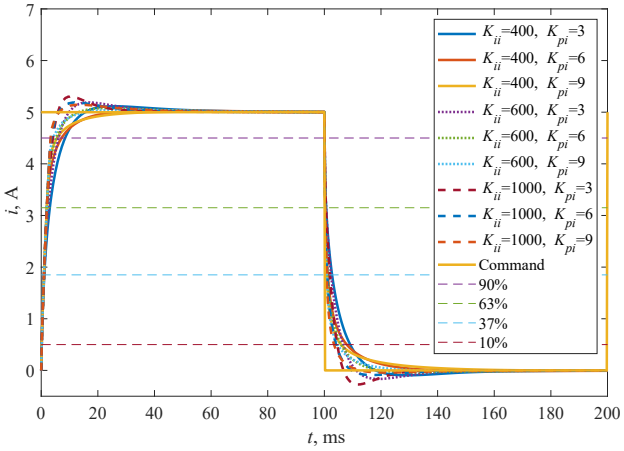

Fig. 7. Closed loop: response to current step inputs – coil current, I_{cmd} =5 A

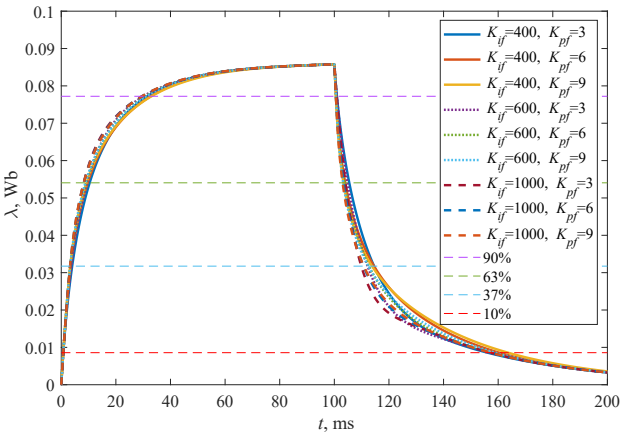

Fig. 8. Closed loop: response to current step inputs – flux, I_{cmd} =5 A

Maxwell. In either case, the control scheme was implemented in Twin Builder, whereas the actuator was modelled in Ansys Maxwell. The control system model was then driven by the prescribed current commands (current controller) or the flux command signals. Throughout the course of the simulations the controllers' settings were varied to choose adequate gains for the two control systems. The results are highlighted in the sections below.

A. Open loop

First, consider the open loop system response to voltage step inputs (excitation frequency – 5 Hz, duty cycle – 50 %). The actuator's response was simulated over the 200 ms time span. The voltage was varied to result in the peak coil currents from 1 up to 5 A. The outcome is illustrated in Figs. 5 to 6. Note that although the current circuit's first-order (63%) response times are below 20 ms, the current output does not reach steady-state within 100 ms. That is even more evident when analyzing the magnetic flux time histories in Fig. 6.

B. Current PI controller

In this section we reveal the response of an MR control system with the current driver as in Fig. 3. The system's response was simulated using the same excitation input as in the previous case. To study the impact of proportional gain (K_{pi}) and the integral gain (K_{ii}), the PI controller's settings were varied throughout the simulations. Specifically, the proportional gain K_{pi} was within the range from 3 to 9, and the integral gain K_{ii} was altered from 400 to 1000. The results are highlighted in Fig. 7. However, as demonstrated in Figs. 9 and 10, although the current circuit's response time has been considerably improved, the flux still lags behind the current, and zero flux could not be achieved for another 100 ms despite the current being zero.

C. Cascade controller

This section reveals the results obtained using the cascade controller as in Fig. 4. The results can be observed in Figs. 11 to 12. In particular, the control system model was subjected to magnetic flux step inputs λ_{cmd}. For the ease of comparison, the step function parameters were similar to the waveform used in the open loop and the current driver cases, respectively, i.e. Λ_{cmd} =0.075 Wb, frequency – 5 Hz, duty cycle – 50%. Based on the observations of the flux output in Fig. 11 the cascade controller is efficient in driving the flux to zero, thus effectively

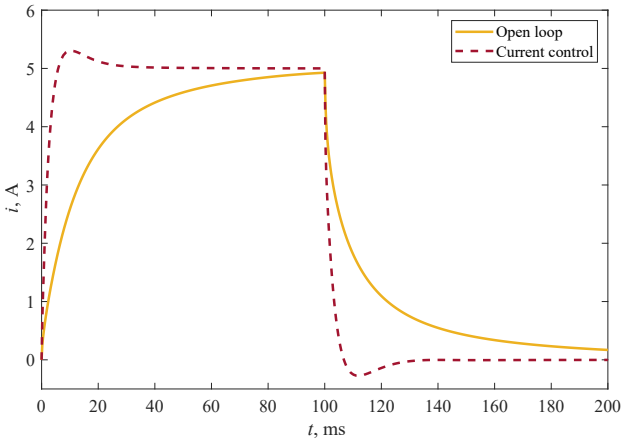

Fig. 9. Coil current response comparison: uncontrolled vs controlled; I_{cmd} =5 A

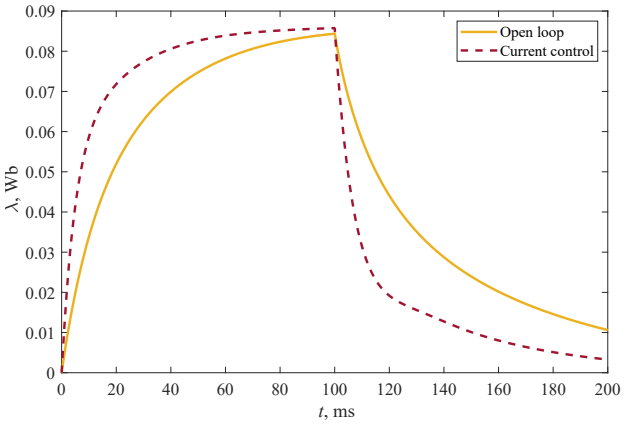

Fig. 10. Flux response comparison: uncontrolled vs controlled; I_{cmd} =5 A

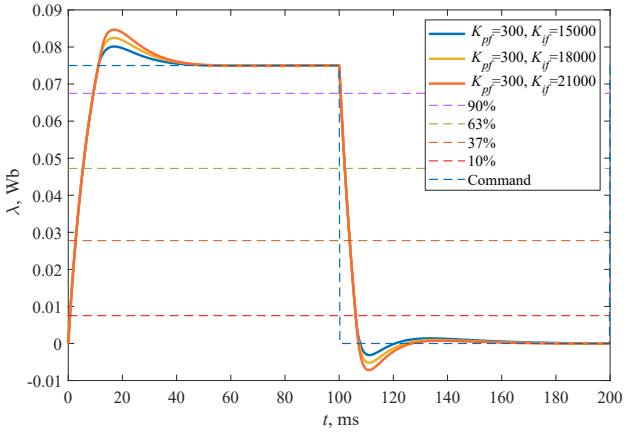

Fig. 11. Cascade controller: flux response to flux step inputs; Λ_{cmd} =0.075 Wb, current driver: K_{pi} =40, K_{ii} =4000

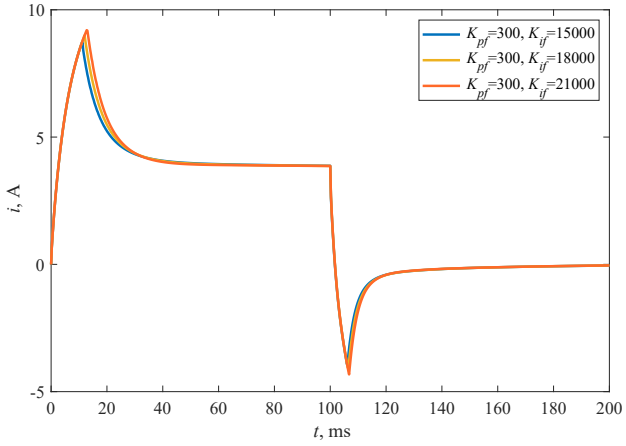

Fig. 12. Cascade controller: current response to flux step inputs; Λ_{cmd} =0.075 Wb, current driver: K_{pi} =40, K_{ii} =4000

reducing any unwanted effects due to the eddy currents in the structure. The controller was tuned in a similar manner as in the previous case with the current driver gains set to K_{pi} =40, K_{ii} =4000, K_{pf}=300 and K_{if} varied from 15000 to 21000. It is evident that the cascade controller is significantly faster in every aspect.

V. Summary and Conclusions

In this paper we present the results of simulations highlighting major differences between a conventional PID controller with a current feedback loop and one that involves a controller driven by flux feedback. To realize this study, we developed a hybrid model of the MR actuator, and then performed a parametric study using various control system variants. It is apparent then that the cascade controller is superior to the current one as it is capable of driving the magnetic flux to zero which is not possible for the conventional (current) drivers. Moreover, the approach improves the response time of the actuator. We plan to include other important phenomena (magnetic hysteresis, temperature, mechanical loads) as well as to further optimize the control scheme.

Acknowledgment

This research had received funding from the National Agency for Academic Exchange (NAWA Poland) grant no. PPI//APM/2018/1/00027/DEC/1.

References

[1] J. Rabinov, "The magnetic field clutch," *AIEE Trans.*, vol. 67, pp. 1308–1315, 1948.

[2] J. Gołdasz, B. Sapiński, Ł. Jastrzebski, and M. Kubik, "Dual hysteresis model of MR dampers," *Frontiers in Materials*, vol. 7, p. 236, 2020.

[3] Z. Strecker, I. Mazurek, J. Roupec, and M. Klapka, "Influence of MR damper response time on semiactive suspension control efficiency," *Meccanica*, vol. 50, no. 8, pp. 1949–1959, 2015.

[4] M. Kubík, O. Macháček, Z. Strecker, J. Roupec, and I. Mazurek, "Design and testing of magnetorheological valve with fast force response time and great dynamic force range," *Smart Materials and Structures*, vol. 26, no. 4, p. 047002, 2017.

[5] S.-B. Choi, W. Li, M. Yu, H. Du, J. Fu, and P. X. Do, "State of the art of control schemes for smart systems featuring magneto-rheological materials," *Smart Materials and Structures*, vol. 25, no. 4, p. 043001, 2016.

[6] S. Guo, S. Li, and S. Yang, "Semi-active vehicle suspension systems with magnetorheological dampers," in *2006 IEEE International Conference on Vehicular Electronics and Safety*. IEEE, 2006, pp. 403–406.

[7] S.-B. Choi, H. Lee, S.-R. Hong, and C. Cheong, "Control and response characteristics of a magnetorheological fluid damper for passenger vehicles," in *Smart Structures and Materials 2000: Smart Structures and Integrated Systems*, vol. 3985. SPIE, 2000, pp. 438–443.

[8] H. Pang, F. Liu, and Z. Xu, "Variable universe fuzzy control for vehicle semi-active suspension system with MR damper combining fuzzy neural network and particle swarm optimization," *Neurocomputing*, vol. 306, pp. 130–140, 2018.

[9] S.-B. Choi *et al.*, "Design of a new adaptive fuzzy controller and its application to vibration control of a vehicle seat installed with an MR damper," *Smart Materials and Structures*, vol. 24, no. 8, p. 085012, 2015.

[10] S. Gad, H. Metered, A. Bassuiny, and A. Abdel Ghany, "Multi-objective genetic algorithm fractional-order PID controller for semi-active magnetorheologically damped seat suspension," *Journal of Vibration and Control*, vol. 23, no. 8, pp. 1248–1266, 2017.

[11] T. Nehl, S. Gopalakrishnan, and F. Deng, "Direct flux control for magnetic structures," Patent EP1 868 214B1, 2006.

[12] G. Yang, *Large-scale magnetorheological fluid damper for vibration mitigation: modeling, testing and control*. University of Notre Dame, 2002.

[13] T. Nehl, C. Namuduri, A. Omekanda, and S. Gopalakrishnan, "Actuator with integrated flux sensor," Patent 9,657,699, 2017.